U.S. DEPARTMENT OF THE INTERIOR
U.S. GEOLOGICAL SURVEY

TO ACCOMPANY OPEN-FILE REPORT 98–494

GEOLOGIC MAP OF THE ALDER CREEK QUADRANGLE, MALHEUR COUNTY, OREGON

By James G. Evans[1] and G. Benjamin Binger[2]

INTRODUCTION

The Alder Creek quadrangle is located about 60 km southwest of the town of Vale, Malheur County, Oregon (figure 1). The quadrangle can be reached from U.S. Highway 20 by a graded county road that goes south from the Harper turn-off on U.S. 20. Numerous jeep trails provide access from the county road to most parts of the quadrangle.

The formations of the quadrangle were originally named and described by Kittleman and others (1965). A reconnaissance geologic map (scale 1:63,360) that includes the quadrangle was made by Hagood (1963) as part of a study of the Monument Peak area. Hagood's mapping was incorporated into a geologic map of the Owyhee region at the scale of 1:125,000 (Kittleman and others, 1967), a geologic map of eastern Oregon at the scale of 1:500,000 (Walker, 1977), and a geologic map of the State of Oregon at the scale of 1:500,000 (Walker and MacLeod, 1991). The geology of the Alder Creek quadrangle was mapped at the scale of 1:24,000 in 1991 as part of a cooperative project between the Oregon Department of Geology and Mineral Industries and the U.S. Geological Survey. The geology was incorporated into the geologic map of the Vale 30 by 60 minute quadrangle (Ferns and others, 1993) at the scale of 1:100,000.

The chemical classification of the volcanic rocks used in this report is based on the total alkali-silica diagram of Le Bas and others (1986). The correspondence between absolute ages and geologic ages is from Palmer (1983).

The rocks exposed in the Alder Creek quadrangle mostly comprise a flat-lying to gently dipping section of volcanic, pyroclastic, and volcaniclastic rocks of late Tertiary age. The quadrangle is located along the western margin of the north-trending, 50 x 100 km, middle Miocene Oregon-Idaho graben (Ferns and others, 1993). The western margin of the graben is generally placed where the stratigraphy changes abruptly from the early to middle Miocene largely flood basalt-rhyolite volcanic rock association of the western horst to the middle to late Miocene sedimentary, pyroclastic, and silicic to intermediate volcanic rocks of the graben. This structural and stratigraphic transition zone is located about 2 km west of the eastern boundary of the Alder Creek quadrangle.

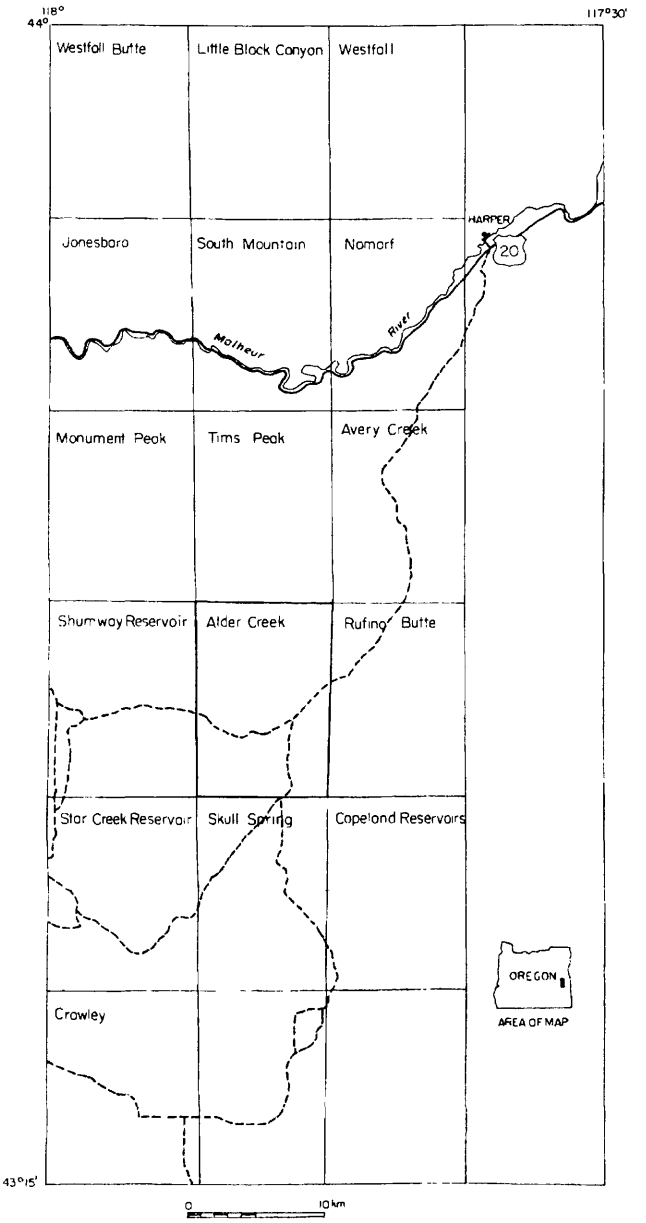

Figure 1. Index map showing locations of the Alder Creek quadrangle (bold outline) and other quadrangles mentioned in this report. The solid lines are paved roads. The dashed lines are dirt roads.

[1]U.S. Geological Survey, Spokane, Wash.
[2]Washington State University, Pullman, Wash.

Manuscript approved for publication September 9, 1998.

STRATIGRAPHY

The oldest unit of the horst, the early to middle Miocene basalt of Malheur Gorge (map unit Tm, Evans, 1990a,b), is exposed along parts of Camp, Cottonwood, and Skull Creeks. The name "basalt of Malheur Gorge" as used here is equivalent to part of the "unnamed igneous complex" of Kittleman and others (1965). This thick sequence of tholeiitic basalt flows is petrologically, stratigraphically, and geochemically equivalent to the Imnaha and Grande Ronde Basalt of the Columbia River Basalt Group (Binger, 1997). These flows of the basalt of Malheur Gorge, however, probably did not erupt from the dike swarms that fed the Columbia River Basalt Group to the north. A vent for the basalt of Malheuer Gorge is located in the Jones Butte area, 10 km to the northwest (Evans, 1996). The basalt flows are coarsely porphyritic along Camp and Cottonwood Creeks and resemble the lower part of the formation in the Malheur Gorge area (Evans, 1990a,b; sample A, table 2), 12 km to the north, where as much as 600 m of the formation are exposed. (A short unlabelled segment of Camp Creek is in sec. 28, T. 22 S., R. 40 E.) The flows along Skull Creek are finer grained, sparsely phyric and aphyric, consist of basalt (sample J, table 2), and generally resemble the upper part of the formation in the Malheur Gorge area. The basalt was dated at 16.8±1.2 Ma, 16.9±0.67 Ma, 17.9±1.76 Ma, and 18.5±1.37 Ma ($^{40}Ar/^{39}Ar$ method; Lees, 1994; Lees' samples KL-91-49, KL-91-80, KL-91-164, and KL-92-231). These dates are generally consistent with the ages of the Imnaha, Picture Gorge, and Grande Ronde Basalts of the Columbia River Basalt Group (Baksi, 1989).

The Dinner Creek Welded Tuff (map unit Td; Greene and others, 1972; formerly the Dinner Creek Welded Ash-Flow Tuff of Kittleman and others, 1965) overlies the basalt of Malheur Gorge in the northwestern part of the quadrangle and forms cliffs as much as 5 m high formed by the strongly welded uppermost part of the formation. The less strongly welded parts of the formation below the cliffs consist of generally white bedded tuff. Although the bulk of the formation in the quadrangle is not welded, no formation name change is proposed in this report. The formation ranges in thickness from 30 to 80 m in the quadrangle. The Dinner Creek in the quadrangle differs from Dinner Creek to the north, which has a persistent central strongly welded member and lapilli tuff of variable thickness above and below the welded tuff. In the Monument Peak area (Evans, 1996) and along parts of Malheur Gorge (Evans, 1990b), the lapilli tuff is absent and the welded tuff is 3 to 6 m thick, or is absent. Average composition of the Dinner Creek is alkali rhyolite (Haddock, 1967; Evans, 1990a, table 1; table 2, this report, samples N and R). Based on his estimate of the increase in thickness of the Dinner Creek to the west-northwest, Haddock (1967) suggested that the vent from which the tuff was erupted is at Castle Rock, about 55 km northwest of the quadrangle. However, recent mapping (M.L. Cummings, Portland State University, unpub. mapping, 1996) indicates that Castle Rock is not a vent. The thickness of the Dinner Creek in the Westfall Butte quadrangle (Evans and Binger, 1997a) about 40 km to the north-northwest appears to increase greatly to the north of Westfall Butte and suggests a vent source in that direction. A northerly provenance of the unit is further suggested by the northerly increase in lithic fragments in the strongly welded part of the formation near Westfall Butte from a few percent to as much as 50 percent. A possible Dinner Creek vent north of Westfall Butte is buried by younger rocks. K-Ar radiometric ages of the Dinner Creek in Malheur Gorge are 15.3±0.4 and 14.7±0.4 Ma (K-Ar method, Fiebelkorn and others, 1983). Based on these radiometric ages, the age of the Dinner Creek is about 15 Ma, or middle Miocene.

The Hunter Creek Basalt (map unit Th; Kittleman and others, 1965; Greene and others, 1972) overlies the Dinner Creek Welded Tuff. The Hunter Creek resembles the uppermost part of the basalt of Malheur Gorge in being black, generally aphyric, and containing rare sedimentary interbeds. Chemically, the Hunter Creek Basalt north of the quadrangle is an icelandite (Carmichael, 1974; typical Hunter Creek contains Al_2O_3=Fe_2O_3=14%), or a basaltic andesite (Le Bas and others, 1986; Evans, 1990a,b). In the Alder Creek quadrangle, the basaltic andesite above the Dinner Creek is continuous with Hunter Creek mapped in the adjacent Tims Peak quadrangle (Evans and Keith, 1996) to the north. Two lines of evidence strongly suggest that, although the Hunter Creek Basalt is younger than Dinner Creek based on its stratigraphic position over the Dinner Creek, the flows erupted relatively soon after the Dinner Creek Welded Tuff was emplaced. A lens of black vitrophyre in the Dinner Creek in the Jonesboro quadrangle (Evans, 1990a, table 1) has an icelandite composition like that of the icelandite magma type of the Hunter Creek Basalt, suggesting mingling between rhyolite and icelandite magmas prior to eruption of the Dinner Creek. In sec. 34 and 35, T. 12 S., R. 39 E. in the Westfall Butte quadrangle (Evans and Binger, 1998), the dominantly rhyolitic tuff of the Dinner Creek grades to andesitic tuff just below the Hunter Creek flows. Intrusion of the Hunter Creek magma into the Dinner Creek magma chamber may have triggered eruption of the Dinner Creek as a result of rapid increase of pressure in the upper part of the chamber. For this reasons the Hunter Creek is assigned a middle Miocene age, probably very close in age to the Dinner Creek. Lees ($^{40}Ar/^{39}$ Ar method, 1994; Lees' samples HOR-9, KL-91-100, KL-91-102, KL-92-269, and KL-92-278) dated Hunter Creek at 15.0±0.73, 15.8±0.6, 15.9±0.26, 16.5±1.2, and 18.6±0.63 Ma. The youngest date is most in accord with the hypothesis that the Hunter Creek was erupted shortly after the eruption of the Dinner Creek Welded Tuff.

The Littlefield Rhyolite (map unit Tlr; Kittleman and others, 1965; samples S and U, table 2) overlies Hunter Creek Basalt and is remarkable for its regional extent (1,100 km^2) and volume (100 km^3). The unit is generally about 100 m thick where it is part of a flat-lying stratigraphic sequence in

the northwestern part of the quadrangle and may be part of a rhyolite dome where its exposed thickness is greater than 100 m (maximum more than 215 m) in the central part of the quadrangle. The central part of the quadrangle also has elevated aeromagnetic intensity (figure 3), which suggests a great thickness of the magnetite-rich rhyolite, possibly in the form of a vent under the dome. Lees ($^{40}Ar/^{39}Ar$ method, 1994; Lees' samples KL-91-46, KL-91-47, and KL-92-258) dated Littlefield Rhyolite in the Namorf quadrangle (Ferns and O'Brien, 1992) 20 km to the north at 15.2±0.31, 16.3±0.87, and 16.8±0.4 Ma. The youngest date is most in accord with radiometric dates of underlying map units.

The area mapped as Littlefield Rhyolite in the south-central part of the quadrangle contains basaltic andesite that could be part of the older Hunter Creek Basalt (sample F, table 2; field identification of the rock was rhyolite). Inasmuch as it was not identified as a separate unit in the field, the basaltic andesite may be a large xenolith in Littlefield Rhyolite, a small intrusion, or it may constitute a basaltic andesite flow between rhyolite flows.

Tuffaceous sandstone (map unit Tts), sandstone (map unit Tss), and sedimentary and pyroclastic rocks (map unit Tsp) overlie Littlefield Rhyolite and are largely differentiated in the field by the volcanic rock units that overlie them. Tuffaceous sandstone is overlain by the trachyandesite flow (map unit Tta); sandstone, by the Wildcat Creek Welded Ash-Flow Tuff (map unit Tw); and the sedimentary and pyroclastic unit, by the Shumway Ranch Basalt (map unit Tsr) and the welded tuff (map unit Twt). Where trachyandesite is not present the sandstone unit may contain the older tuffaceous sandstone. Where the trachyandesite and Wildcat Creek are not present, the sedimentary and pyroclastic rocks unit, Tsp, may include one or both sandstone units.

The trachyandesite flow (map unit Tta) in sec. 18, T. 23 S., R. 40 W. underlies Wildcat Creek Welded Ash-Flow Tuff (map unit Tw) and the sedimentary and pyroclastic rocks unit (map unit Tsp) and overlies tuffaceous sandstone (map unit Tts). The occurrences of this unit are limited to a few fault blocks in the west-central part of the Alder Creek quadrangle and the adjacent part of the Shumway Reservoir quadrangle to the west. The 2 to 3 percent K_2O in analyzed rock may be in potassium feldspar in the groundmass, or the feldspar may be ternary. Some of the unit's chemistry may be the result of hydrothermal alteration. The unit represents a small volume lava flow, possibly an intracanyon flow, the vent of which may be a possible east-west-striking dike located along the line between secs. 19 and 30, T. 23 S., R. 40 E.

The Wildcat Creek Welded Ash-Flow Tuff (map unit Tw; Kittleman and others, 1965) may have erupted from a 1.2-km-long, north-trending dike 8.5 km to the southwest in the Star Creek Reservoir quadrangle (Evans, unpub. mapping, 1992). Because of its varied appearance, seven samples of the welded tuff were analyzed for major oxides; six of them are rhyolitic and one is dacitic in composition (samples G to I, L, Q, T, and V, table 2). Some of the lithologic and geochemical variation of the welded tuff may be due to the variable amount of partly digested to undigested fragments of fine-grained hematite-rich basalt. Similar variability in composition in the Wildcat Creek is reported by Ferns and Williams (1993) in the Crowley quadrangle, 15 km to the southwest.

Unit Twt, the youngest welded ash-flow tuff, resembles a welded tuff mapped in the Little Black Canyon 7.5' quadrangle (Evans and Binger, 1997b), 40 km to the north. In the Alder Creek quadrangle the welded tuff overlies the sedimentary and pyroclastic rocks unit (map unit Tsp) and underlies the middle Miocene Shumway Ranch Basalt (map unit Tsr) in SE1/4 sec. 27, T. 23 S., R. 40 E. This ash flow may have been erupted from a vent at or near the Westfall Butte volcanic center 50 km to the northwest (Evans and Binger, 1997a). Brooks and O'Brien (1992) and Ferns and others (1993, their map unit Ttdv) mapped a welded tuff that may correlate with the unit Twt, in the Westfall quadrangle, 50 km to the northeast. Their welded tuff unit, Ttdv, overlies the Bully Creek Formation and was assigned to the upper Miocene based on the interpretation that the relatively high zirconium content of the ash-flow tuff identifies it as upper Miocene (9.2 Ma) Devine Canyon Ash-Flow Tuff of Greene and others (1972). Binger (1997) drew the same conclusion from geochemical data. An upper Miocene age, however, is uncertain because these welded tuffs in the Little Black Canyon, Westfall Butte, Westfall, and Alder Creek quadrangles do not resemble the Devine Canyon Ash-Flow Tuff (Twt, crystal -poor; Devine Canyon, crystal-rich), some exposures of it underlie middle Miocene Shumway Ranch Basalt, and the unit has not yet been dated. A middle Miocene age of Twt in the Alder Creek quadrangle can be inferred from stratigraphic relations (middle Miocene Shumway Ranch Basalt over Twt). The presence of partly digested mafic volcanic fragments argues for a more local vent source for Twt, perhaps the same as for the Wildcat Creek, and against Twt as a distal facies of the Devine Canyon.

The stratigraphic units along the eastern margin of the quadrangle are at the western margin of the Oregon-Idaho graben (Ferns and others, 1993). They include the rhyolite of Dry Creek, a basaltic andesite unit, and sedimentary and pyroclastic rocks of the Oregon-Idaho graben. The rhyolite of Dry Creek, informally named here, in the southeastern corner of the quadrangle is the oldest of these map units to judge by the mapping of Brooks (his unit Tdr_2, 1992a,b) in the adjacent Rufino Butte and Copeland Reservoir quadrangles where the rhyolite is at least 150 m thick.

The basaltic andesite flows exposed in the southeastern part of the quadrangle along Dry Creek (map unit Tba) correlate with the basaltic andesite in the adjacent Rufino Butte quadrangle (Brooks, 1992b; his unit Tdb), where it attains a thickness of 150 m and overlies rhyolite continuous with the rhyolite of Dry Creek. The basaltic andesite flows are probably associated with extensional development of the Oregon-

Idaho graben (Ferns and others, 1993) and are of limited volume and extent. The chemical composition of the basaltic andesite in the Alder Creek quadrangle (samples B, D, W, X, and Y, table 2) is similar to the composition of the basaltic andesite in the Rufino Butte quadrangle (Brooks, 1992b; table 4, this report).

The sedimentary and pyroclastic rocks of the Oregon-Idaho graben, map unit Tspo, may be correlative with all or parts of map units Tts, Tss, and Tsp in the horst section. The coarse clasts (maximum 2 m) in the conglomerate and the blocks (maximum 5 m) in the tuff breccia are unusual in the generally fine-grained sedimentary and pyroclastic rocks of the Oregon-Idaho graben. Their location close to the western margin of the graben suggests rapid subsidence and filling of the graben and a nearby vent-source for the tuff breccia. Apparently, the later subsidence also involved the horst, which acted as a platform within a regional subsidence regime. A laminated welded tuff like the one comprising most of the clasts of the conglomerate was found about 12 km to the southwest in the southwest corner of the Star Creek Reservoir quadrangle (Evans, unpub. mapping, 1992), which is the closest known source of these clasts. Clasts of this kind were found to the north in the southeastern part of the adjacent Tims Peak quadrangle (Evans and Keith, 1996). Blocks of sandstone and siltstone in the tuff breccia indicate that sediments had accumulated in the area affected by the pyroclastic eruptions. The granodiorite fragment found in the tuff breccia may be from the magma chamber.

The entire exposed section of the Oregon-Idaho graben sequence in the southeastern corner of the quadrangle and adjacent parts of the Rufino Butte quadrangle is about 365 m thick. Based on geophysical modeling of geophysical data, however, Griscom and Halvorson (unpub. data, 1995) suggest that the graben has abrupt geophysical boundaries that correspond well with vertical projections of the surface faults and is about 2 km deep. Therefore, only a small part of the late subsidence history of the graben in the Alder Creek area is revealed in exposures, as the top of the flood-basalt basement is estimated to be at an elevation of -2,100 ft (cross section A-A'). Consequently, it is likely that the graben section exposed in the quadrangle is upper middle Miocene, and this age assignment is tentatively accepted in this report.

The Shumway Ranch Basalt (Kittleman and others, 1965; samples E and K, table 2) is the only exposed volcanic rock that is found both on the horst and in the Oregon-Idaho graben; it is correlative with map unit Tsb of Brooks (1992b) in the adjacent Rufino Butte quadrangle (see analyses of samples E and K in table 1 and samples 302 and 304 in table 4). The distribution of the basalt suggests that the graben-horst boundary had little topographic expression in late middle Miocene. The present topographic expression is a result of differential erosion.

Alluvial fan deposits (map unit QTf) that preserve fan morphology are found in the southwestern part of the quadrangle. They could be as old as late Miocene or as young as Quaternary.

Landslide deposits (map unit Qls) are found mostly along north-trending faults, especially where basalt overlies poorly lithified sedimentary rocks. The largest deposits are along part of Cottonwood Creek and along northern Red Butte and the western flank of the mesa of Shumway Ranch Basalt in the northeastern part of the quadrangle; each of these deposits covers about 2.5 km^2.

Alluvium (map unit Qa) is found along Camp, Cottonwood, Cherry, Alder, Dry, and Skull Creeks.

METAMORPHISM AND (OR) HYDROTHERMAL ALTERATION

Most of the map units from basalt of Malheur Gorge to the alluvial fan deposits show evidence of low-grade metamorphism and (or) hydrothermal alteration in thin section; these two processes of mineralogical change may not be easily differentiated where neomineralization is incipient, as in the study area. Plagioclase is altered to sericite and epidote, especially in the basaltic andesite flows. Clinopyroxene and olivine are altered to biotite and actinolite, especially in the basalt of Malheur Gorge and the basaltic andesite flows. Mafic minerals are altered to biotite as high up in the section as the Shumway Ranch Basalt. Sericite, some of it coarse enough to be called muscovite, is present as a cement in the sedimentary and pyroclastic rocks, including the alluvial fan deposits. The only intrusion suspected to be in the quadrangle is the proposed feeder for the Littlefield Rhyolite flows and a related dome in the central part of the quadrangle. This intrusion could not have supplied the heat required to cause thermal metamorphism or hydrothermal alteration in map units younger than the Littlefield Rhyolite and possibly also adjacent units of the Oregon-Idaho graben. It is possible that the more intense mineralogical changes in the basalt of Malheur Gorge and the basaltic andesite flows of the Oregon-Idaho graben section are largely related to intrusion of Littlefield Rhyolite and that subsequently unrelated hydrothermal systems along the western margin of the graben and connecting faults, account for the widespread paleothermal effects. Alternatively, the thermal effects could be due in part to the late Miocene silicic volcanism to the southwest in the Crowley area (Ferns and Williams, 1993). Evidence of hydrothermal activity as late as Quaternary in the horst was found to the northwest in the Monument Peak quadrangle (Evans, 1996).

STRUCTURE

The quadrangle contains two different stratigraphic sections that consist of flat-lying to gently dipping volcanic and sedimentary rocks that reflect eruption of flood-basalt in early to middle Miocene and formation of the north-trending, 50 x 100 km, middle Miocene Oregon-Idaho graben as a result of

east-west extension. The stratigraphic sections are in contact along a north-northeast-striking fault zone near the eastern margin of the quadrangle.

The contact between the two sections roughly parallels the transition between the regionally relatively high gravity potential characteristic of the Oregon-Idaho graben and the lower gravity potential of the horst (Griscom and Halvorson, unpub data, 1995; figure 2; cross-section A-A'). The western margin of the Oregon-Idaho graben is shown in figure 2 by a north-northeast-trending line of stippled hot-dogs. Although generally the graben shows relatively high areomagnetic intensity, in the segment of the graben margin included in the quadrangle, the aeromagnetic high reflects an intrusion of Littlefield Rhyolite along the horst-graben contact (Griscom and Halvorson, 1994; figure 3). The Littlefield Rhyolite exposed in the central part of the quadrangle is interpreted as a north-northeast-trending intrusion that extends from about sec. 2, T. 23 S., R. 40 E. to about sec. 34, same township. The persistent high aeromagnetic intensity in the northwestern part of the quadrangle is at least partly attributable to the 100- to 150-m-thick Littlefield Rhyolite flows which tend to be relatively highly magnetic.

Most faults in the quadrangle have northerly strikes that vary between north-northeast to north-northwest, but are generally subparallel to the western margin of the Oregon-Idaho graben.

The north-northwest-trending line of stippled hot-dogs

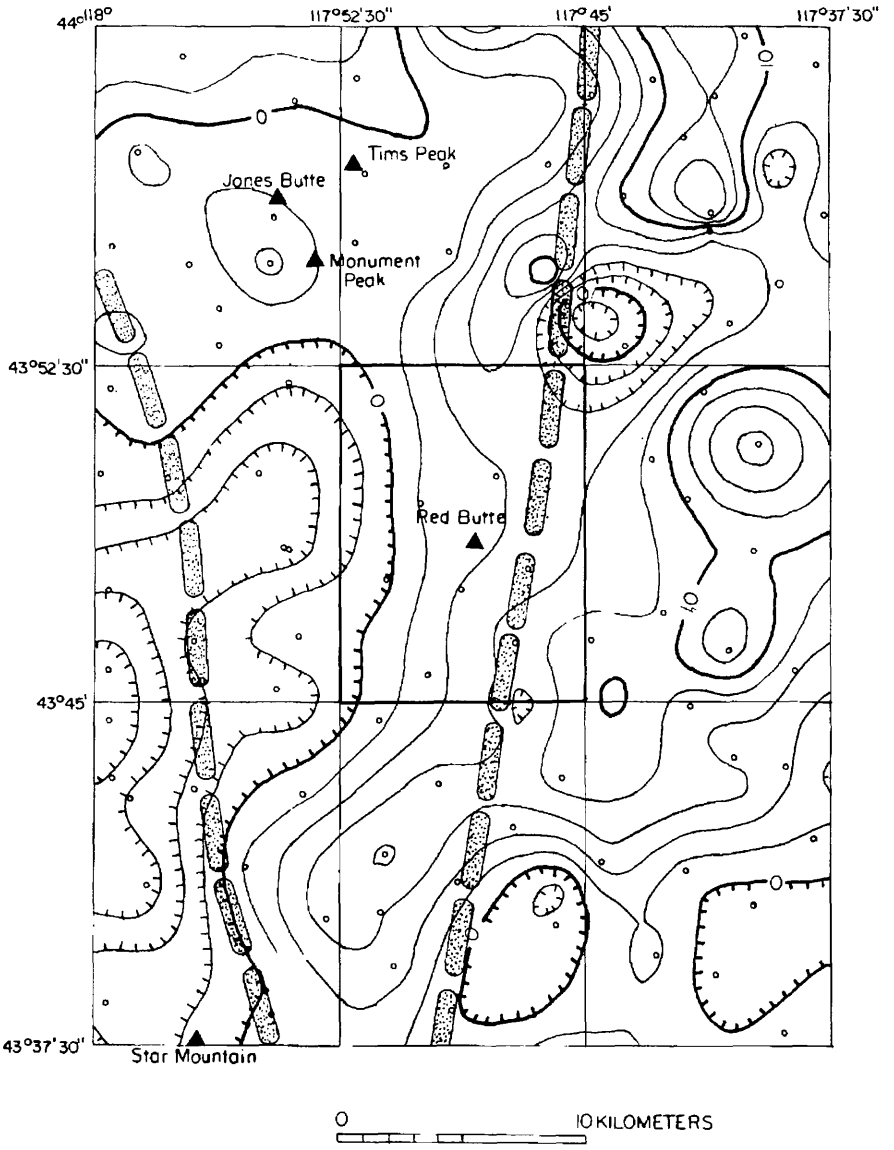

Figure 2. Isostatic residual gravity anomaly map of the Alder Creek (bold outline) and adjacent quadrangles. Modified from Griscom and Halvorson (1994). Contour interval 2 milligals. Hachures indicate closed lows. Stippled hot-dogs mark the western margin (fault zone) of the Oregon-Idaho graben (NNE) and the western margin of the horst (NNW). See figure 1 for names of quadrangles adjacent to Alder Creek quadrangle.

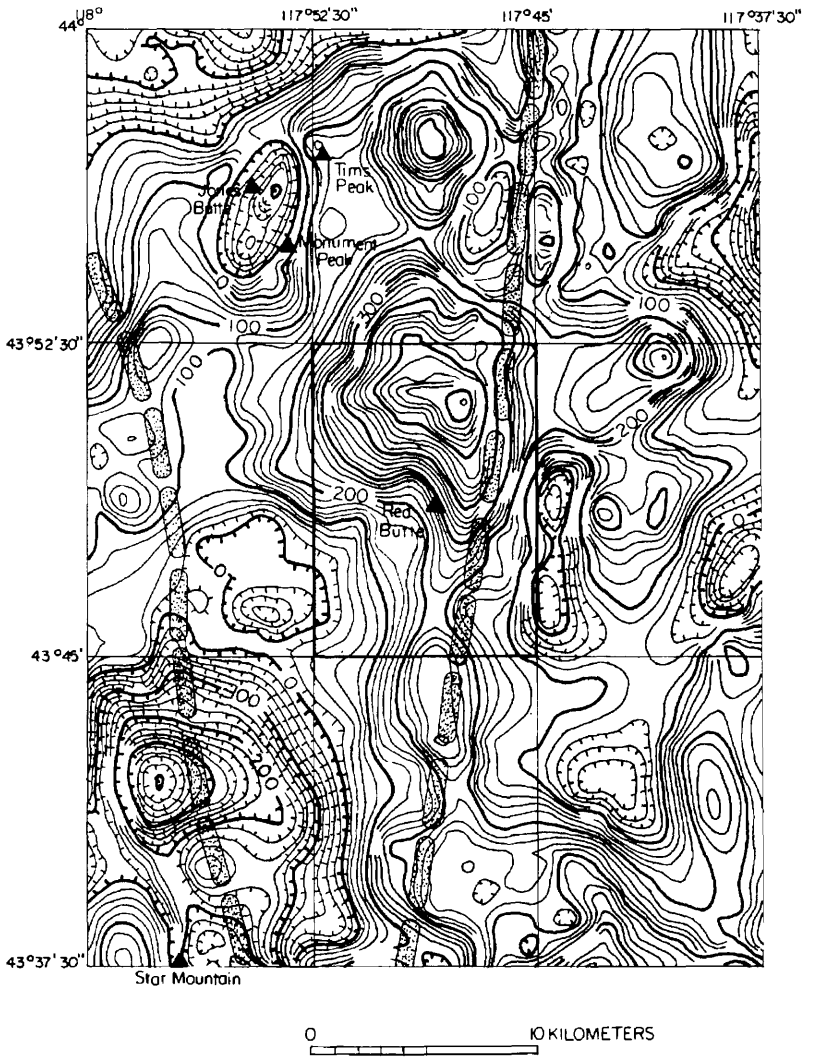

Figure 3. Aeromagnetic map of the Alder Creek (bold outline) and adjacent quadrangles. Modified from Griscom and Halvorson (1994). Contour interval 20 and 100 nanoteslas. Hachures indicate closed lows. The stippled hot-dogs are aligned along the western margin (fault zone) of the Oregon-Idaho graben (NNE) and the western margin of the horst (NNW). See figure 1 for names of quadrangles adjacent to the Alder Creek quadrangle.

west of the quadrangle (figures 2 and 3) marks the approximate western margin of the horst. West of that line is another graben and associated Stockade Mountain silicic volcanic center (Walker and MacLeod, 1991). The graben may be part of the Juntura Basin of Shotwell (1963).

GEOCHEMISTRY

Twenty-five unaltered volcanic rocks and nine altered rocks were collected for analysis by James G. Evans. Of the unaltered rocks, three were analyzed by the U.S. Geological Survey (samples A, B, and C) for major elements using wave-length dispersive x-ray fluorescence spectroscopy (Taggart and others, 1990) and for major and minor elements by inductively coupled plasma atomic emission spectrometry (Briggs, 1990); 12 samples were analyzed for major and 17 minor elements by x-ray spectroscopy (Hooper and others, 1990) by G.B. Binger at the GeoAnalytical Laboratory, Washington State University, Pullman (samples D to O); and 10 samples were analyzed for major and 12 minor elements by Bondar-Clegg (samples P to Y). These results are shown in table 3.

Samples A, B, and C were analyzed for the following trace elements, which were not found at the lower limits of detection indicated in parentheses and are not shown in table 3: silver (<2 ppm), arsenic, (<10 ppm), gold (<8 ppm), bismuth (<10 ppm), cadmium (<2 ppm), holmium (<4 ppm), molybdenum (<2 ppm), tin (<5 ppm), and uranium (<100 ppm).

The altered rocks were analyzed by the U.S. Geological Survey for 31 major and trace elements by the inductively coupled plasma atomic emission spectrometry method (Briggs, 1990), and the data are reported in table 7. How-

ever, the following elements are not included in table 7 because they occur in uniformly low concentrations in all samples: silver, bismuth, cadmium, holmium, molybdenum, tin, and uranium. The samples were analyzed for gold by the flame and graphite-furnace atomic absorption spectrophotometry method (O'Leary, 1990), but no gold was detected at the lower limit of detection of 0.002 ppm. Mercury was analyzed by the cold-vapor atomic absorption spectrophotometry method (O'Leary and others, 1990) and the results are shown in table 7.

The altered rocks and siliceous veins are high in hematite and (or) high in silica in the form of chalcedony and opal veins. Iron content ranges from 0.75 to 22 weight percent; the highest concentration was found in hematite-cemented siltstone (sample 643) in map unit Tsp.

The significance of trace-element concentrations in the altered rocks and veins is revealed by comparison with concentrations of the same elements in the unaltered rocks and to crustal abundances. Because the unaltered rocks were analyzed for different suites of trace elements at each of the three laboratories, the analyses are not complete enough for comparison of all trace elements. In addition, analytical procedures are different enough at each of the laboratories, that direct comparison of semi-quantitative trace-element data from the laboratories is inaccurate in general. However, in this study, the data are assumed to suggest general trends in trace-element data. The unaltered rock samples analyzed are divided into sets defined by the trace elements for which they were analyzed. The sets defined in this way consist of 3, 13, 15, 18, 22, 25, and 34 samples (includes analyses of rocks from Rufino Butte quadrangle in table 5). It should also be kept in mind that the terms "altered" and "unaltered" are relative, and some of the freshest rocks submitted for whole-rock analysis may have sustained addition or subtraction of trace elements without showing outward signs of post-emplacement alteration. In general we assume that the freshest-looking rocks best preserve primary chemical composition.

Based on the lack of sufficient chemical data, the following trace elements can be dismissed from further discussion: beryllium, europium, gallium, manganese, neodymium, and ytterbium. Arsenic and mercury fit the criterion here for lack of data for comparison because they were only analyzed at the USGS laboratory, and mercury was only analyzed in the altered rocks. However, arsenic and mercury are common in hydrothermal systems in the region and are generally considered significant at detectable levels of greater than or equal to 10 ppm for arsenic and 0.02 ppm for mercury.

Based on comparison of trace elements from sets of 3, 13, 15, 18, 22, 25, or 34 unaltered rocks, trace elements that are at approximately background for the quadrangle are barium, cerium, cobalt, chromium, copper, lanthanum, lithium, niobium, nickel, lead, scandium, strontium, thorium, vanadium, and zinc.

In summary, arsenic and mercury are the only trace elements that can be attributed to hydrothermal activity in the quadrangle. It is suspected, however, that the relatively high trace-element values of arsenic, copper, manganese, scandium, vanadium, and zinc in the hematite-cemented sedimentary rocks (map units Tss, Tsp, and Tspo) are significant because such rocks would generally be expected to contain very low concentrations of these trace elements. Although unaltered-looking sedimentary rock from these map units was not analyzed, their typical lack of hematite cement is expected to correlate with relatively low concentrations for metals and rare earths. Brecciated rhyolite tends to have trace-element concentrations toward the high end of the range in the altered rocks, but not much greater than concentrations in the unaltered rocks.

Gold or silver was not detected in any of the samples (lower limits of detection 0.002 ppm and 0.2 ppm, respectively).

The hydrothermal effects in the alluvial fan deposits, map unit QTf, were not suspected during field work, and, therefore, no samples were taken for minor-element analysis from this map unit. In light of thin section evidence of hydrothermal alteration in the unit, analyses of these deposits for precious metals and other trace elements would be of interest.

In summary, visibly altered volcanic or sedimentary rocks are not abundant in the quadrangle. Samples of brecciated Littlefield Rhyolite and hematite-cemented clastic rocks showed elevated metal and rare-earth concentrations that did not include silver and gold. The brecciated rhyolite occurs along fault zones and is, therefore, narrowly localized. The hematite-cemented sedimentary rocks could be distally and (or) laterally related to paleohydrothermal systems. Some of the mineralization is associated directly or indirectly with east-west, middle Miocene extension.

REFERENCES CITED

Baksi, A.K., 1989, Reevaluation of the timing and duration of extrusion of the Imnaha, Picture Gorge, and Grande Ronde Basalts of the Columbia River Basalt Group, *in* Reidel, S.P. and Hooper, P.R., eds., Volcanism and tectonism in the Columbia River flood-basalt province: Geological Society of America Special Paper 239, p. 105-111.

Binger, G.B., 1997, The volcanic stratigraphy of the Juntura region, eastern Oregon: Pullman, Washington State University, Master's thesis, 206 p.

Briggs, P.H., 1990, Elemental analysis of geological materials by inductively coupled plasma atomic emission spectrometry, *in* Arbogast, B.F., ed., Quality assurance manual for the Branch of Geochemistry: U.S. Geological Survey Open-File Report 90-668, p. 83-91.

Brooks, H.C., 1992a, Preliminary geologic map of the Copeland Reservoir quadrangle, Malheur County, Oregon: Oregon Department of Geology and Mineral Industries Open-File Report O-93-3, scale 1:24,000.

——— 1992b, Preliminary geologic map of the Rufino Butte quadrangle, Malheur County, Oregon: Oregon Department of Geology and Mineral Industries Open-File Map O-92-17, scale 1:24,000.

Brooks, H.C., and O'Brien, J.P., 1992, Geology and mineral resources map of the Westfall quadrangle, Malheur County, Oregon: Or-

egon Department of Geology and Mineral Industries Geological Map Series GMS-71, scale 1:24,000.

Carmichael, I.S.E., 1964, The petrology of Thingmuli, a Tertiary volcano in eastern Iceland: Journal of Petrology, v. 5, p., 435-460.

Evans, J.G., 1990a, Geology and mineral resources map of the Jonesboro quadrangle, Malheur County, Oregon: Oregon Department of Geology and Mineral Industries Geological Map Series GMS-66, scale 1:24,000.

——— 1990b, Geology and mineral resources map of the South Mountain quadrangle, Malheur County, Oregon: Oregon Department of Geology and Mineral Industries Geological Map Series GMS-67, scale 1:24,000.

——— 1996, Geologic map of the Monument Peak quadrangle, Malheur County, Oregon: U.S. Geological Survey Miscellaneous Field Studies Map MF-2317, scale 1:24,000.

Evans, J.G., and Binger, G.B., 1997a, Geologic map of the Westfall Butte quadrangle, Malheur County, Oregon: U.S. Geological Survey Open-File Report 97-491, scale 1:24,000.

——— 1999, Geologic map of the Little Black Canyon quadrangle, Malheur County, Oregon: U.S. Geological Survey Open-File Report 98-493, scale 1:24,000.

Evans, J.G., and Keith, W.J., 1996, Geologic map of the Tims Peak quadrangle, Malheur County, Oregon: U.S. Geological Survey Miscellaneous Field Studies Map MF-2316, scale 1:24,000.

Ferns, M.L., Brooks, H.C., Evans, J.G., and Cummings, M.L., 1993, Geologic map of the Vale 30 x 60 minute quadrangle, Malheur County, Oregon, and Owyhee County, Idaho: Oregon Department of Geology and Mineral Industries Geologic Map Series GMS-77, scale 1:100,000.

Ferns, M.L., and O'Brien, J.P., 1992, Geology and mineral resources of the Namorf quadrangle, Malheur County, Oregon: Oregon Department of Geology and Mineral Industries Geological Map Series GMS-74, scale 1:24,000.

Ferns, M.L., and Williams, Christopher, 1993, Preliminary geologic map of the Crowley quadrangle, Malheur County, Oregon: Oregon Department of Geology and Mineral Industries Open-File Report O-93-4, scale 1:24,000.

Fiebelkorn, R.B., Walker, G.W., MacLeod, N.S., McKee, E.H., and Smith, J.G., 1983, Index to K-Ar determinations for the State of Oregon: Isochron/West, no. 37, p. 3-60.

Greene, R.C., Walker, G.W., and Corcoran, R.E., 1972, Geologic map of the Burns quadrangle, Oregon: U.S. Geological Survey Miscellaneous Investigations Map I-680, scale 1:250,000.

Haddock, G.H., 1967, The Dinner Creek Welded Ash-Flow tuff of the Malheur Gorge area, Malheur County, Oregon: Eugene, University of Oregon, Ph. D. dissertation, 111 p.

Hagood, A.R., 1963, Geology of the Monument Peak area, Malheur County, Oregon: Eugene, University of Oregon, Master's thesis, 165 p.

Hooper, P.R., Johnson, D.M., and Conrey, R.M., 1993, Major and trace element analyses of rocks and minerals by automated X-ray spectrometry: Pullman, Washington State University, Geology Department, Open-File Report, 36 p.

Le Bas, M.J., LeMaitre, R.W., Streckeisen, A., and Zanettin, B., 1986, A chemical classification of volcanic rocks based on the total alkali-silica diagram: Journal of Petrology, v. 27, pt. 3, p. 745-750.

Lees, K.R., 1994, Magmatic and tectonic changes through time in the Neogene volcanic rocks of the Vale area, Oregon, northwestern USA: Milton-Keynes, United Kingdom, The Open University, Ph.D. dissertation, 284 p.

Kittleman, L.R., Green, A.R., Haddock, G.H., Hagood. A.R., Johnson, A.M., McMurray, J.M., Russell, R.G., and Weeden, D.A., 1967, Geologic map of the Owyhee region, Malheur County, Oregon: Eugene, University of Oregon Museum of Natural History Bulletin 8, scale 1:125,000.

Kittleman, L.R., Green, A.R., Hagood, A.R., Johnson, A.M., McMurray, J.M., Russell, R.G., and Weeden, D.A., 1965, Cenozoic stratigraphy of the Owyhee region, southeastern Oregon: University of Oregon Museum of Natural History Bulletin 1, 45 p.

O'Leary, R.M., 1990, Determination of gold in samples of rock, soil, stream sediment, and heavy mineral concentrates by flame and graphite furnace atomic absorption spectrophotometry following dissolution by HB and Br_2, *in* Arbogast, B.F., ed., Quality assurance manual for the Branch of Geochemistry: U.S. Geological Survey Open-File Report 90-668, p. 46-51.

O'Leary, R.M., Crock, J.G., and Kennedy, K.R., 1990, Determination of mercury in geological materials by continuous flow cold vapor atomic absorption spectrophotometry, *in* Arbogast, B.F., ed., Quality assurance manual for the Branch of Geochemistry: U.S. Geological Survey Open-File Report 90-668, p. 60-67.

Palmer, A.R., 1983, The Decade of North American Geology 1983 geologic time scale: Geology, v. 11, no. 9, p. 503-504.

Shotwell, J.A., 1963, Miocene mammalian faunas of southeastern Oregon: University of Oregon Museum of Natural History Bulletin, v. 14, p. 1-67.

Taggert, J.E., Jr., Bartel, Ardith, and Siems, D.F., 1990, High-precision major element analysis of rocks and minerals by wave-length dispersive x-ray fluorescence spectroscopy, *in* Arbogast, B.F., ed., Quality assurance manual for the Branch of Geochemistry, USGS: U.S. Geological Survey Open-File Report 90-668, p. 166-172.

Walker, G.W., 1977, Geologic map of Oregon east of the 121st meridian: U.S. Geological Survey Miscellaneous Geologic Investigations Map I-902, scale 1:500,000.

Walker, G.W., and MacLeod, N.S., 1991, Geologic map of Oregon: Reston, Va., U.S. Geological Survey, scale 1:500,000

Table 1. Locations of unaltered rock samples.

Sample No.	Map unit	Location
A	Tm	SW1/4 sec. 28,T. 22 S., R.40 E.
B	Tba	S1/2 sec. 25, T. 23 S., R. 40 E.
C	Tlr	NE1/4 sec. 5, T. 23 S., R. 40 E.
D	Tba	NW1/4 sec. 25, T. 23 S., R. 40 E.
E	Tba	same
F	Tlr	NW1/4 sec. 3, T. 24 S., R. 40 E
G	Tw	NW1/4 sec. 19, T. 23 S., R. 40 E.
H	Tw	NW1/4 sec. 4, T. 24 S., R. 40 E.
I	Tw	SW1/4 sec. 4, T. 24 S., R. 40 E.
J	Tm	S1.2 sec. 4, T. 24 S., R. 40 E.
K	Tsr	SE1/4 sec. 17, T. 23 S., R. 40 E.
L	Tw	NE1/4 sec. 17, T. 23 S., R. 40 E.
M	Tta	NW1/4 sec. 18, T. 23 S., R. 40 E.
N	Td	SW1/4 sec. 4, T. 23 S., R. 40 E.
O	Th	SW1/4 sec. 28, T. 22 S., R. 40 E.
P	Tta	Near NW corner sec. 4, T. 23 S., R. 40 E.
Q	Tw	SE1/4 sec. 18, T. 23 S., R. 40 E.
R	Td	Near NE corner sec. 5, T. 23 S., R. 40 E.
S	Tlr	Near Se corner sec. 8, T. 23 S., R. 40 E.
T	Tw	S1/2 sec. 19, T. 23 S., R. 40 E.
U	Tlr	SE1/4 sec. 4, T. 24 S., R. 40 E.
V	Tw	SW1/4 sec. 3, T. 24 S., R. 40 E.
W	Tba	SW1/4 sec. 24, T. 23 S., R. 40 E.
X	Tba	same
Y	Tba	SE1/4 sec. 2, T. 24 S., R. 40 E.

Table 2. Major oxide analyses of unaltered rock samples listed in table 1.

[Normalized on a volatile-free basis. Samples A to C were analyzed by X-ray spectroscopy by the U.S. Geological Survey and Total iron is reported as Fe_2O_3. Samples D to O were analyzed at the WSU GeoAnalytical Laboratory and total iron is reported as FeO. Samples P to Y were analyzed by Bondar-Clegg and iron is reported as Fe_2O_3 and FeO]

Sample No.	A	B	C	D	E	F	G	H	I	J	K
Map unit	Tm	Tba	Tlr	Tba	Tsr	in Tlr	Tw	Tw	Tw	Tm	Tsr
Rock name	basalt	basaltic andesite	dacitic welded tuff	basaltic andesite	basaltic andesite	basaltic andesite	rhyolite	dacite	rhyolite	basalt	basaltic trachy-andesite
Oxides											
SiO_2	51.11	53.37	67.71	55.15	54.66	55.97	72.28	64.87	73.90	51.86	52.45
Al_2O_3	16.83	16.82	14.72	16.89	16.91	13.59	13.27	13.85	12.66	14.21	16.73
Fe_2O_3	11.90	9.48	7.29								
FeO				7.67	8.05	12.14	3.22	9.17	2.67	13.91	10.50
MgO	4.50	5.20	0.93	4.73	4.85	3.22	0.27	0.30	0.04	4.21	3.89
CaO	10.02	8.51	3.84	8.40	8.28	6.92	0.83	2.61	0.47	8.76	7.96
Na_2O	2.67	3.43	2.29	3.78	3.84	3.26	3.73	4.34	5.29	3.14	3.86
K_2O	0.62	1.31	1.40	1.41	1.43	1.86	5.81	3.13	4.57	0.65	1.62
TiO_2	1.87	1.23	1.05	1.309	1.315	2.377	0.385	1.257	0.255	2.467	2.038
P_2O_5	0.28	0.49	0.66	0.502	0.513	0.458	0.098	0.381	0.027	0.549	0.79
MnO	0.19	0.16	0.11	0.153	0.159	0.202	0.116	0.079	0.124	0.245	0.157

Sample No.	L	M	N	O	P	Q	R	S	T	U	V
Map unit	Tw	Tta	Td	Th	Tta	Tw	Td	Tlr	Tw	Tlr	Tw
Rock name	rhyolite	trachy-andesite	rhyolite	basaltic andesite	trachy-andesite	rhyolite	rhyolite	rhyolite	rhyolite	rhyolite	rhyolite
Oxides											
SiO_2	72.94	57.67	75.27	52.91	62.55	72.79	77.30	72.29	75.83	71.10	72.92
Al_2O_3	13.33	17.11	12.80	15.47	12.77	12.82	11.70	12.42	10.76	12.21	12.76
Fe_2O_3					5.15	3.21	1.86	5.14	1.25	6.41	3.16
FeO	2.92	7.53	2.38	10.32	5.66	0.20	0.02	0.12	1.81	0.00	0.09
MgO	0.14	3.05	0.56	5.34	1.00	0.38	0.21	0.31	0.17	0.36	0.41
CaO	0.44	6.41	0.85	9.41	4.07	0.36	0.29	0.73	0.25	0.77	0.40
Na_2O	5.39	4.11	2.71	3.35	4.14	5.41	4.79	4.38	4.48	4.37	5.32
K_2O	4.27	2.00	5.10	0.89	2.88	4.30	3.56	4.05	5.12	4.10	4.41
TiO_2	0.373	1.456	0.209	1.811	1.21	0.35	0.20	0.43	0.23	0.41	0.32
P_2O_5	0.113	0.529	0.066	0.284	0.36	0.06	0.04	0.08	0.03	0.08	0.08
MnO	0.078	0.134	0.069	0.215	0.21	0.12	0.03	0.05	0.07	0.19	0.13

Sample No.	W	X	Y
Map unit	Tba	Tba	Tba
Rock name	basaltic andesite	basaltic andesite	basaltic andesite
Oxides			
SiO_2	54.04	54.62	54.357
Al_2O_3	16.83	16.60	16.543
Fe_2O_3	4.44	6.43	9.320
FeO	4.82	3.15	0.000
MgO	4.60	4.04	4.932
CaO	8.70	8.41	8.436
Na_2O	3.49	3.49	2.877
K_2O	1.32	1.38	1.695
TiO_2	1.28	1.37	1.243
P_2O_5	0.48	0.51	0.442
MnO	0.00	0.00	0.154

Table 3. Major- and trace-element analyses of unaltered rock samples listed in table 1.

Concentrations of Al, Ca, Fe, K, Mg, Na, P, and Ti in samples A to C are in weight-percent; concentrations of other elements are in parts per million (ppm). Samples A to C were analyzed by inductively coupled plasma atomic emission spectroscopy by the U.S. Geological Survey. Samples D to O were analyzed for 17 trace-elements by X-ray fluorescence at the WSU Geoanalytical Laboratory. Samples P to Y were analyzed for 12 trace-elements by Bondar-Clegg]

Sample No.	A	B	C
Map unit	Tm	Tba	Tlr
Elements			
Al	8.7	8.9	7.3
Ca	6.7	5.9	2.6
Fe	7.7	6.4	4.7
K	0.51	1.1	1.0
Mg	2.6	3.0	0.55
Na	2.3	2.7	1.7
P	0.12	0.22	0.28
Ti	1.2	0.69	0.58
Ba	330	660	950
Be	<1	1	2
Ce	23	45	56
Co	38	33	11
Cr	110	120	9
Cu	140	63	28
Ga	23	20	20
La	15	25	32
Li	12	12	10
Mn	1,400	1,200	750
Nb	7	6	10
Nd	26	30	34
Ni	45	71	5
Pb	<4	7	14
Sc	33	27	17
Sr	350	510	270
Th	4	4	6
V	330	230	46
Y	31	25	46
Yb	3	2	5
Zn	92	87	150

Sample No.	D	E	F	G	H	I	J	K	L	M	N	O
Map unit	Tba	Tsr	in Tlr	Tw	Tw	Tw	Tm	Tsr	Tw	Tta	Td	Tba
Elements												
Ni	42	43	0	11	0	9	6	28	12	10	13	41
Cr	84	87	17	8	0	0	26	72	3	19	0	106
Sc	29	46	36	6	22	1	33	37	3	27	4	40
V	249	242	371	17	35	0	447	260	28	204	8	343
Ba	743	789	808	1,065	1,308	610	541	1,034	1,064	1,523	1,317	481
Rb	20	19	50	95	88	104	16	16	92	30	74	20
Sr	481	492	323	53	287	12	366	592	47	533	46	405
Zr	157	162	201	398	328	424	188	193	392	212	404	133
Y	27	28	43	73	46	68	42	37	75	38	88	31
Nb	11.2	11.3	17.4	30.8	26.0	33.4	12.8	16.2	30.2	17.7	28.1	8.1
Ga	19	20	21	24	27	21	23	25	25	22	22	21
Cu	63	49	0	3	0	6	96	31	7	24	6	63
Zn	88	89	133	127	144	128	133	119	121	96	147	100
Pb	6	4	9	15	14	16	2	5	15	8	19	6
La	19	21	17	44	40	55	13	30	60	35	32	17
Ce	49	48	61	98	73	102	47	56	118	56	99	45
Th	3	0	5	7	7	11	9	1	7	4	8	3

Sample No.	P	Q	R	S	T	U	V	W	X	Y
Map unit	Tta	Tw	Td	Tlr	Tw	Tlr	Tw	Tba	Tba	Tba
Elements										
Cr	0	12	12	0	19	0	13	107	69	144
Co	12	0	0	5	0	5	5	32	27	33
Ni	7	0	0	0	0	0	7	66	54	78
Cu	2	5	1	1	4	2	9	71	85	71
Zn	167	108	116	154	240	165	129	97	99	71
Rb	94	99	74	139	142	127	120	0	0	33
Sr	261	60	23	150	0	166	51	0	0	525
Y	62	101	93	84	209	105	120	30	17	33
Zr	503	476	602	1,330	598	505	147	180	130	389
Nb	32	53	31	62	111	56	45	20	19	40
Ba	1,370	1,720	1,690	2,170	93	2,240	1,680	774	876	785
Li	16	16	4	26	44	24	22	11	12	9

Table 4. Normalized major oxide analyses of selected unaltered rock samples from the Rufino Butte quadrangle for comparison with major oxide analyses of unaltered rocks from the Alder Creek quadrangle.

[Map unit symbols are the ones used by Brooks (1992). Tsb=Tsr, this report; Tdr_2= Trdc, this report; Tbd=Tba, this report]

Sample No.	302	304	328	329	340	323	330	331	335
Map unit	Tsb	Tsb	Tdr_2	Tdr_2	Tdr_2	Tdb	Tdb	Tdb	Tdb
Rock name	trachy-basalt	trachy-basalt	rhyolite	rhyolite	rhyolite	basaltic trachy-andesite	trachy-andesite	basaltic andesite	basaltic trachy-andesite
Oxides									
SiO_2	51.81	51.38	72.79	71.67	75.58	53.78	61.74	53.22	54.35
Al_2O_3	16.14	16.10	14.40	14.71	12.97	15.68	15.70	15.86	16.17
Fe_2O_3	5.03	5.63	1.84	0.53	1.27	10.87	6.07	10.70	10.54
FeO	6.32	6.22	0.25	1.44	0.12				
MgO	4.60	4.71	0.00	0.47	0.17	3.99	2.98	4.40	3.63
CaO	8.08	8.10	1.33	1.30	0.44	7.91	4.85	9.01	7.80
Na_2O	3.47	3.50	4.29	4.55	4.21	3.68	3.82	3.44	3.78
K_2O	1.64	1.48	4.72	4.92	4.94	1.60	3.34	1.18	1.53
TiO_2	2.00	1.98	0.38	0.41	0.22	1.64	1.08	1.53	1.49
P_2O_5	0.74	0.72	0.00	0.00	0.05	0.67	0.31	0.49	0.53
MnO	0.17	0.18	0.00	0.00	0.03	0.18	0.10	0.17	0.17

Table 5. Trace-element analyses of selected unaltered rocks from the Rufino Butte quadrangle for comparison with trace-element analyses from the Alder Creek quadrangle.

[Map unit symbols are the ones used by Brooks (1992)]

Sample No.	302	304	328	329	340	323	330	331	335
Map unit	Tsb	Tsb	Tdr_2	Tdr_2	Tdr_2	Tdb	Tdb	Tdb	Tdb
Elements									
Cr	73	81	47	11	0	56	65	520	45
Co	28	32	0	6	0	28	20	31	28
Ni	46	54	10	5	5	34	39	40	35
Cu	49	53	8	9	7	85	31	67	64
Zn	127	130	3	36	33	110	70	102	98
Rb	18	36	0	0	0	0	0	0	0
Sr	610	616	153	147	27	481	304	518	472
Y	37	39	13	30	34	28	41	20	36
Zr	197	213	319	327	289	171	234	153	171
Nb	14	26	31	41	37	23	0	52	25
Ba	1,030	1,740	1,390	1,180	763	940	838	697	720
Li	10	10	20	35	17	10	56	8	14

Table 6. Descriptions and locations of altered rock and vein samples.

Sample No.	Map unit	Description	Location
638	Tspo	Hematite-enriched tuffaceous sandstone	W1/2 sec. 36, T. 23 S., R. 40 E
639	Tba	White chalcedony veins	Near center sec. 1, T. 24 S., R. 40 E.
640	Trdc	Chalcedony-cemented rhyolite breccia	SE1/4 sec. 1, T. 24 S., R. 40 E.
641	Tlr	Oxidized and brecciated rhyolite	SE1/4 sec. 23, T. 23 S., R. 40 E.
642	Tss	Hematite-cemented siltstone	NE1/4 sec. 28. T. 23 S., R. 40 E.
643	Tsp	Hematite-enriched siltstone	Near SE corner sec. 21, T. 23 S., R. 40 E.
644	Tlr	White chalcedony	NE1/4 sec. 9, T. T. 24 S, R. 40 E.
645	Tm	Chalcedony veins	SW1/4 sec. 4, T. 24 S., R. 40 E.
646	Tlr	Brecciated rhyolite	SW1/4 sec. 4, T. 23 S., R. 40 E.

Table 7. Major- and trace-element analyses of altered rock and vein samples listed in table 4.

[Concentrations of Al, Ca, Fe, K, Mg, Na, P, and Ti are in weight-percent. Concentrations of other elements are in ppm. "<" followed by a number means that the element was present in concentrations less than the lower confidence limit indicated]

Sample No.	638	639	640	641	642	643	644	645	646
Map unit	Tspo	Tba	Trdc	Tlr	Tss	Tsp	Tlr	Tm	Tlr
Elements									
Al	5.1	0.97	6.8	6.6	5.0	4.7	0.10	1.4	6.2
Ca	1.5	0.58	0.85	0.81	1.2	1.2	0.04	0.56	1.8
Fe	14	0.75	1.3	4.5	18	22	2.9	0.51	6.8
K	1.2	0.20	3.6	2.3	1.3	0.23	0.04	0.23	2.1
Mg	0.78	0.23	0.19	0.43	0.53	1.1	0.03	0.21	0.24
Na	0.72	0.25	2.3	2.0	0.83	0.31	0.02	0.03	2.5
P	0.17	0.04	0.05	0.02	0.12	0.11	0.01	0.06	0.17
Ti	0.27	0.07	0.19	0.31	0.30	0.27	<0.005	0.04	0.60
As	70	<10	<10	<10	50	110	20	<10	<10
Ba	1,700	120	840	1,600	780	560	54	620	1,100
Be	4	<1	2	3	5	7	<1	<1	1
Ce	64	5	57	110	63	72	<4	<4	83
Co	18	5	3	14	9	19	<1	2	8
Cr	13	10	3	17	15	18	<1	4	1
Cu	17	31	8	17	110	150	2	8	4
Eu	<2	<2	<2	2	<2	<2	<2	<2	2
Ga	18	7	18	24	15	20	<4	<4	22
Hg	0.20	0.16	0.10	0.03	0.04	0.06	N0.02	0.05	0.02
La	34	3	38	60	31	22	<2	3	44
Li	10	30	18	20	14	28	3	4	13
Mn	7,800	270	240	1,000	1,100	3,900	120	110	890
Nb	11	<4	11	25	13	13	<4	<4	16
Nd	29	<4	26	54	30	22	<4	<4	44
Ni	12	8	2	23	20	26	<2	3	<2
Pb	10	<4	16	18	6	5	<4	<4	12
Sc	8	3	5	10	11	11	<2	<2	20
Sr	180	50	170	140	180	160	6	210	260
Th	5	<4	14	11	<4	<4	<4	<4	8
V	380	16	18	180	530	810	22	33	5
Y	38	3	27	75	44	46	<2	4	51
Yb	6	<1	3	7	6	7	<1	<1	5
Zn	79	14	26	140	150	230	15	10	120